COMMUNICATION

Multicycle water vapour stability of microporous breathing MOF aluminium isophthalate CAU-10-H

Dominik Fröhlich,[a,b] Stefan Kai Henninger*[a] and Christoph Janiak*[b]

The hydrothermal stability of aluminium hydroxide isophthalate MOF CAU-10-H was proven, under humid multi-cycling conditions. Detailed *in situ* thermogravimetric measurements and *in situ* powder X-ray diffraction analysis during water ad-/desorption were used. A reversible structural change during adsorption was detected and thereby exemplified the robustness of breathing-like MOFs over 700 water vapour ad/desorption cycles. In combination with high water adsorption capacity, hydrophilic CAU-10-H is the first breathing-like MOF with a structural change which is a promising candidate for the use in heat transformation processes.

Metal–organic frameworks (MOFs) receive continuous attention due to their high potential for various applications[1] based on their designable and high microporosity.[2] With this new generation of porous materials, significant improvements in gas storage,[3] separation processes,[4] or sorption based heat transformation applications[5] are possible. Thermally driven systems like adsorption chillers (AC), adsorption heat pumps (AHP) or solid desiccant cooling (SDC) are gaining more and more attention as a promising approach to energy efficient heating and cooling.[6,7] However, the relatively low stability under non-inert conditions, especially the often poor long-lasting water vapour stability of MOFs is a critical issue for numerous industrial processes. With regard to the use in ACs, AHP and SDC and their inherent sorption processes, the water vapour stability must be guaranteed over several thousand up to hundreds of thousand cycles. Although several MOFs are claimed as moisture stable, stability often originates from the hydrophobic character of the compound.[8,9] Typically, water stability tests consist of stirring the material in boiling water.[10] Unfortunately, stability tests with liquid water give no clear evidence regarding the use under water vapour conditions.

Whereas under liquid conditions the pores are instantly completely filled with water which remains there during the whole process, this is not the case for cyclic water vapour sorption processes in which pores get filled and emptied many times. Furthermore, during water ad- and desorption processes a phase change from gaseous to the adsorbed phase accompanied by enthalpy exchange (heat of ad- and desorption) to and from the framework occurs. This leads to additional energetic stress to the coordinative metal–ligand bonds as the enthalpy of ad-/desorption is within the range of the activation energy for ligand displacement. In addition, pore stress due to guest–host hydrogen-bonding interactions accompanied by a possible breathing of the framework can occur.[7] Additionally, thermal stress is applied due to heating and cooling of the materials during the heat transformation process for typical temperatures in the range of 20 up to 150 °C. Thus, the evaluation of the multi-cycle hydrothermal stability is of great importance. At present, it is not clear if 'breathing' MOFs, which undergo a phase transition while ad-/desorption, are sufficiently stable to withstand a large number of gas sorption cycles in the presence of water vapour.

'Breathing' in MOFs refers to the motion of a flexible framework adapting to guest molecules, that is, a reversible swelling or shrinking with atomic displacements which can reach several Å.[11] The most famous 'breathing' MOF is MIL-53 which adapts a large pore and a narrow pore form, depending of the host–guest interactions.[11,12] Therefore, we subjected a hydrophilic breathing-like MOF to multi-cycling experiments with water vapour.

Recently, the development of a series of hydrophilic aluminium MOFs was reported by Stock *et al.*[13] which were tested for their hydrothermal stability by stirring in aqueous media at different pH values and solvothermal conditions. The microporous aluminium isophthalate CAU-10-H (*cf.* Fig. 1) shows a water adsorption isotherm of beneficial s-shape with the main loading lift occurring at a comparatively low relative pressure ($0.15 < p/p_0 < 0.25$) (*cf.* Fig. 2).[13] Especially for the use in heat pump applications, the adsorption at low relative water vapour pressure is of great interest.

[a]*Fraunhofer Institute for Solar Energy Systems ISE, Heidenhofstrasse 2, 79110 Freiburg, Germany. E-mail: Dominik.Froehlich@ise.fraunhofer.de, stefan.henninger@ise.fraunhofer.de; Fax: +49 761 4588913; Tel: +49 761 45885817*
[b]*Institut für Anorganische Chemie und Strukturchemie, Heinrich-Heine-Universität Düsseldorf, Universitätsstr. 1, 40225 Düsseldorf, Germany. E-mail: janiak@uni-duesseldorf.de; Tel: +49 211 8112286*
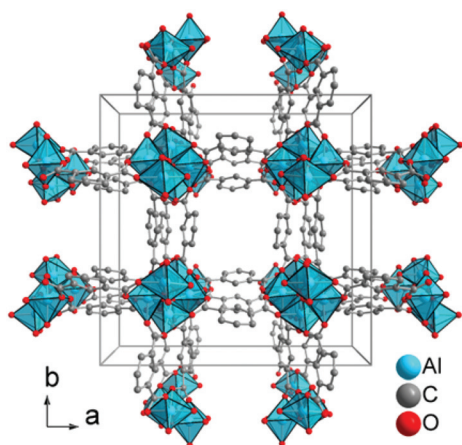
Fig. 1 Section of the packing diagram of CAU-10-H. The structure was redrawn with Diamond[14] using the CIF-file supplied with ref. 13.
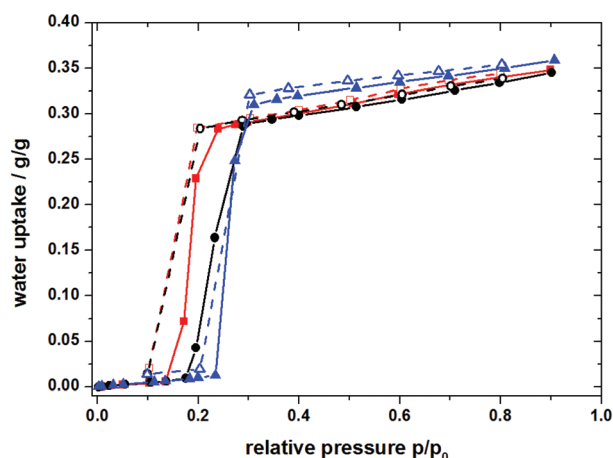

Fig. 2 Water ad-/desorption isotherm of CAU-10-H at different temperatures. 25 °C adsorption ─■─, 25 °C desorption ─ □ ─, 40 °C adsorption ─●─, 40 °C desorption ─ o ─, 60 °C adsorption ─▲─, 60 °C desorption ─ △ ─.

MOFs which were previously investigated for cyclic water sorption processes, such as Cr-MIL-101 showed high absolute water adsorption capacities albeit at a high p/p_0 (>0.7) because of their limited hydrophilicity.[5] With more hydrophilic compounds, the usable loading lift for AC or AHP applications should be shifted to lower p/p_0 (<0.4).

To evaluate the application oriented hydrothermal stability towards water vapour sorption the aluminium isophthalate CAU-10-H was synthesized according to the literature procedure by Stock *et al.*[13] In detail, 200 mg of 1,3-benzenedicarboxylic acid (1,3-H$_2$BDC, 1.20 mmol) dissolved in 1 mL of *N,N*-dimethylformamide (DMF) and 800 mg Al$_2$(SO$_4$)$_3$·18H$_2$O dissolved in 4 mL H$_2$O were placed in a 37 mL Teflon-lined steel-autoclave for 12 h at 135 °C. After cooling to room temperature, the product was filtered and purified by washing three times *via* simultaneous sonication in 10 mL of water. The white solid was first dried for 24 h at 50 °C and afterwards activated for 24 h at 120 °C in vacuum.

Initial water adsorption isotherms where obtained on a *Quantachrome® Hydrosorb*, after vacuum degassing (120 °C/24 h) at 25 °C, 40 °C and 60 °C (*cf.* Fig. 2). Stability to water was tested by *in situ* X-ray analysis under different humidity conditions. Diffractograms were acquired on a Bruker D8 Advanced diffractometer, with Cu-Kα radiation, combined with an MRI TC-humidity chamber, coupled to a humidified nitrogen flow generated by an Ansyco® humidifier. A diffractogram was measured bidirectional at every 5% relative humidity (r.H.) between 0% r.H. and 90% r.H. at a constant temperature of 40 °C (*cf.* Fig. 3). The short time *in situ* thermogravimetric cycling test was performed on a *Setaram™ TGA-DSC-111* with a humidified argon gas flow at 40 °C (*cf.* Fig. 4). The sample temperature was varied between 40 °C and 140 °C, whereas the gas flow temperature and relative humidity was kept constant at 40 °C and 76.3% r.H. corresponding to a water vapour pressure of 5.6 kPa. A fixed-time procedure was used, where a full cycle consisted of a desorption step with heating from 40 °C to 140 °C with a heating rate of 20 K min^{-1} followed by an isothermal step for 90 min for complete desorption and finally cooling down to 40 °C with 20 K min^{-1} where water adsorption takes place. To keep the experiment at a reasonable time scale, equilibrium measurements are only performed for the first and the last cycle, holding the sample at 40 °C for 20 h. Hence the complete experiment with 100 cycles took about 15 days. To expand the hydrothermal stress experiments a newly developed apparatus for powders and granules was used. Two alternating air streams are passed through the
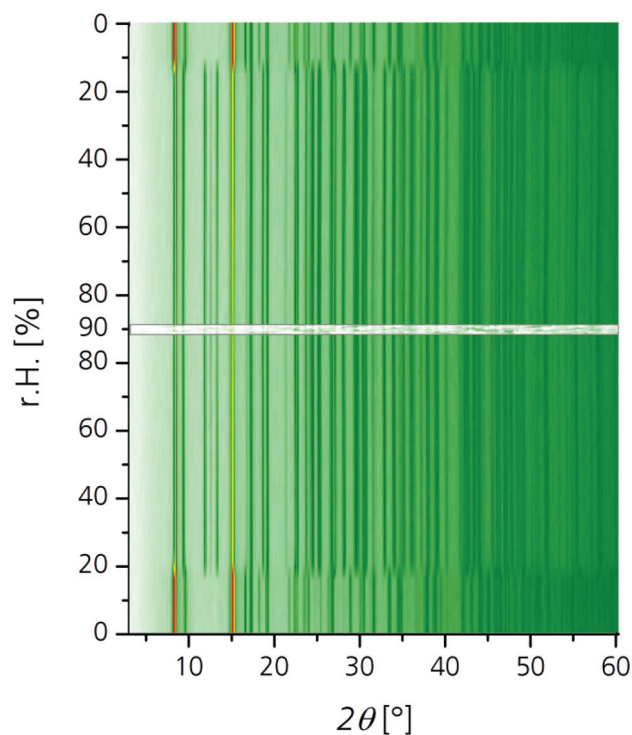

Fig. 3 Powder X-ray diffraction (PXRD) carpet plot showing a reversible structural change upon water ad- and desorption around 20% r.H. (red: high intensity, yellow: middle intensity, green: low intensity).
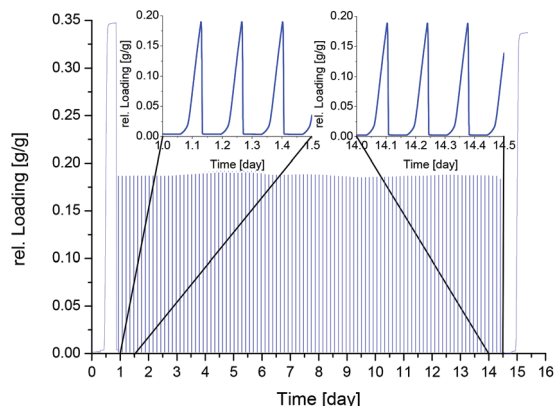
Fig. 4 Thermogravimetric cycling test of CAU-10-H at constant humidity.

Fig. 5 Powder X-ray diffractogram of activated sample (a) and after 700 water sorption cycles (b), both recorded under dry conditions.

sample. Desorption is achieved by a hot air stream at 120 °C at 0% r.H., whereas adsorption is realized with a humidified air stream at 40 °C and 85% r.H. The streams are controlled by mass-flow-controllers and operated at 12 L min^{-1}. This corresponds to a total water impact of 0.4 g H_2O min^{-1} or a water excess of around six times compared to the maximum water uptake of the sample with a cycling time of 20 minutes and a sample amount of around 4 g. This allows faster cycles under open system conditions.

The performed hydrothermal stability tests do not exactly reproduce any particular cycle, but are a good profile of the general underlying temperatures and humidity in open and closed systems. Although, within closed cycle systems, addition stress occurs due to the vacuum or low vapour pressure, we assume that the main weakness is due to the coordinative metal–ligand bonds, which must withstand the repetitive hydrophilic attack of water. This is reflected by the chosen test conditions as a good first approximation.

The specific surface area of CAU-10-H is $S_{BET} = 525$ m^2 g^{-1} (635 m^2 g^{-1} in ref. 13) with a pore volume of 0.27 cm^3 g^{-1} (0.25 cm^3 g^{-1} in ref. 13). The volumetric water sorption isotherms show a sigmoidal shape with a steep rise at a low relative pressure ($0.15 < p/p_0 < 0.25$) (Fig. 2). Adsorption and desorption isotherms were measured at 25 °C, 40 °C and 60 °C. Nearly no hysteresis was observed at 25 °C and 60 °C in our water sorption experiments. However, a slight difference between the adsorption and desorption path for the isotherm measured at 40 °C is visible, which can be directly related to the corresponding phase transition visible within the PXRD experiments.

The diffraction patterns of the *in situ* PXRD at 40 °C show a significant structural change at the step from 15 to 20% r.H. (*cf.* Fig. 3). At this point the positions and the ratio of the intensity of the major reflections change. This can be attributed to a structural change, akin to breathing effects with water as guest molecule similar to MIL-53.[15] The shifts in the reflections at about 20% r.H. correspond to the steep water uptake in the adsorption isotherm. As saturation is achieved at a relative pressure of 25% r.H. the structural change is complete.
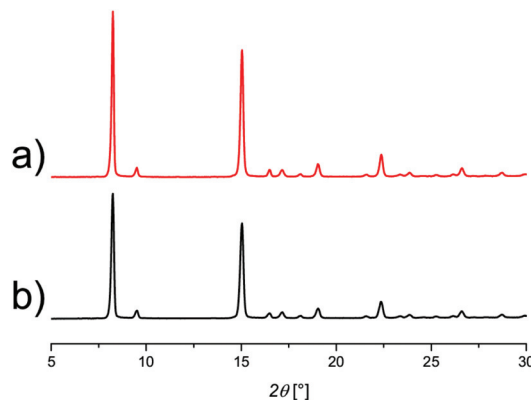
Upon desorption the structure changes back to the initial state at 20% r.H. This coincides excellent with the desorption path of the isotherm, where desorption starts at the same r.H. of $p/p_0 = 0.2$ (Fig. 2). This supports the assumption, that the structural change during ad- and desorption of water is a completely reversible process and structural integrity and crystallinity is preserved. Thus, a good hydrothermal stability for the use in cyclic water sorption applications can be expected.

Based on the good results of the *in situ* PXRD analysis, hydrothermal stability was evaluated by short time *in situ* thermogravimetric cycling tests in a humid atmosphere, as described above (*cf.* Fig. 4). In these experiments, long equilibration times are often needed, because the heat and mass transfer to the sample is limited by thermal coupling and geometry of the crucible. After 100 ad-/desorption cycles, there was no visible change in adsorption dynamics, also the dry weight remained constant. The adsorption capacity remains constant before and after cycling with an uptake at the thermodynamic equilibrium of 0.34 g g^{-1} (Fig. 4 before day 1 and after day 15).

To expand the stability testing CAU-10-H was also exposed to a high excess of water, with a rapid humid gas flow as described above. After 700 ad-/desorption cycles the material was removed and analysed again by PXRD. As can be seen in Fig. 5 no irreversible structural change or degradation was observed.

Conclusions

The MOF CAU-10-H exhibits a fully reversible structural change like a 'breathing' effect upon water ad- and desorption. The water adsorption characteristics of CAU-10-H show a high hydrophilicity with a steep and characteristic s-shaped adsorption isotherm already at a low relative humidity around $p/p_0 = 0.2$.

With regard to possible applications in sorptive heat transformation processes, hydrothermal stability was tested by short and long-term cycle tests. Even after 700 ad-/desorption cycles, no degradation of crystallinity was observed, despite considerable phase transition activity of the material.

It is important to note that the hydrothermal stability of CAU-10-H unlike other MOFs such as ZIF-8 is not achieved by hydrophobicity as CAU-10-H is a hydrophilic MOF.

In summary, the advantageous adsorption characteristics combined with an exceptional hydrothermal stability render the CAU-10-H material suitable for the use in thermally driven heat pumps, chillers or dehumidification applications. Although boundary conditions vary strongly with the specific application closed *versus* open AC/AHP, cooling *versus* heat pump or dehumidification (SDC), the initial multicycle water vapor stability has been proven by this contribution. Thus, corresponding tests which are closer to specific application conditions may now follow.

Acknowledgements

Notes and references

1 C. Janiak, *Dalton Trans.*, 2003, 2781–2804; A. U. Czaja, N. Trukhan and U. Muller, *Chem. Soc. Rev.*, 2009, **38**, 1284–1293; M. J. Prakash and M. S. Lah, *Chem. Commun.*, 2009, 3326–3341; C. Janiak and J. K. Vieth, *New J. Chem.*, 2010, **34**, 2366–2388.

2 J. R. Long and O. M. Yaghi, *Chem. Soc. Rev.*, 2009, **38**, 1213–1214; K. Biradha, *New J. Chem.*, 2010, **34**, 2353–2354; H. C. Zhou, J. R. Long and O. M. Yaghi, *Chem. Rev.*, 2012, **112**, 673–674; S. Kitagawa and S. Natarajan, *Eur. J. Inorg. Chem.*, 2010, 3685–3685.

3 J. R. Li, R. J. Kuppler and H. C. Zhou, *Chem. Soc. Rev.*, 2009, **38**, 1477–1504; M. P. Suh, H. J. Park, T. K. Prasad and D. W. Lim, *Chem. Rev.*, 2012, **112**, 782–835; H. Wu, Q. Gong, D. H. Olson and J. Li, *Chem. Rev.*, 2012, **112**, 836–868; L. J. Murray, M. Dinca and J. R. Long, *Chem. Soc. Rev.*, 2009, **38**, 1294–1314.

4 J.-R. Li, Y. Ma, M. C. McCarthy, J. Sculley, J. Yu, H.-K. Jeong, P. B. Balbuena and H.-C. Zhou, *Coord. Chem. Rev.*, 2011, **255**, 1791–1823; G. Férey, C. Serre, T. Devic, G. Maurin, H. Jobic, P. L. Llewellyn, G. De Weireld, A. Vimont, M. Daturi and J. S. Chang, *Chem. Soc. Rev.*, 2011, **40**, 550–562; H. B. Tanh Jeazet, C. Staudt and C. Janiak, *Dalton Trans.*, 2012, **41**, 14003–14027; K. Hunger, N. Schmeling, H. B. Tanh Jeazet, C. Janiak, C. Staudt and K. Kleinermanns, *Membranes*, 2012, **2**, 727–763; H. B. Tanh Jeazet, C. Staudt and C. Janiak, *Chem. Commun.*, 2012, **48**, 2140–2142; J.-R. Li, J. Sculley and H.-C. Zhou, *Chem. Rev.*, 2012, **112**, 869–932; Z. Zhang, Y. Zhao, Q. Gong, Z. Li and J. Li, *Chem. Commun.*, 2013, **49**, 653–661; B. Zornoza, C. Tellez, J. Coronas, J. Gascon and F. Kapteijn, *Microporous Mesoporous Mater.*, 2013, **166**, 67–78; G. X. Dong, H. Y. Li and V. K. Chen, *J. Mater. Chem. A*, 2013, **1**, 4610–4630.

5 C. Janiak and S. K. Henninger, *Chimia*, 2013, **67**, 419–424; S. K. Henninger, F. Jeremias, H. Kummer and C. Janiak, *Eur. J. Inorg. Chem.*, 2012, 2625–2634; G. Akiyama, R. Matsuda, H. Sato, A. Hori, M. Takata and S. Kitagawa, *Microporous Mesoporous Mater.*, 2012, **157**, 89–93; G. Akiyama, R. Matsuda and S. Kitagawa, *Chem. Lett.*, 2010, **39**, 360–361; F. Jeremias, A. Khutia, S. K. Henninger and C. Janiak, *J. Mater. Chem.*, 2012, **22**, 10148–10151; P. Küsgens, M. Rose, I. Senkovska, H. Fröde, A. Henschel, S. Siegle and S. Kaskel, *Microporous Mesoporous Mater.*, 2009, **120**, 325–330; J. Ehrenmann, S. K. Henninger and C. Janiak, *Eur. J. Inorg. Chem.*, 2011, **2011**, 471–474; Y.-K. Seo, J. W. Yoon, J. S. Lee, Y. K. Hwang, C.-H. Jun, J.-S. Chang, S. Wuttke, P. Bazin, A. Vimont, M. Daturi, S. Bourrelly, P. L. Llewellyn, P. Horcajada, C. Serre and G. Férey, *Adv. Mater.*, 2012, **24**, 806–810; S. K. Henninger, H. A. Habib and C. Janiak, *J. Am. Chem. Soc.*, 2009, **131**, 2776–2777; A. Khutia, H. Urs Rammelberg, T. Schmidt, S. Henninger and C. Janiak, *Chem. Mater.*, 2013, **25**, 790–798; F. Jeremias, V. Lozan, S. Henninger and C. Janiak, *Dalton Trans.*, 2013, **42**, 15967–15973; F. Jeremias, D. Fröhlich, C. Janiak and S. K. Henninger, *RSC Adv.*, 2014, **4**, 24073–24082.

6 Y. I. Aristov, *J. Chem. Eng. Jpn.*, 2007, **40**, 1242–1251; Y. I. Aristov, *Appl. Therm. Eng.*, 2013, **50**, 1610–1618; Y. I. Aristov, *Int. J. Refrig.*, 2009, **32**, 675–686; L. G. Gordeeva, A. Freni, Y. I. Aristov and G. Restuccia, *Ind. Eng. Chem. Res.*, 2009, **48**, 6197–6202; Y. I. Aristov, *J. Chem. Eng. Jpn.*, 2007, **40**, 1242–1251; Y. I. Aristov, M. M. Tokarev, A. Freni, I. S. Glaznev and G. Restuccia, *Microporous Mesoporous Mater.*, 2006, **96**, 65–71; B. Dawoud and Y. Aristov, *Int. J. Heat Mass Transfer*, 2003, **46**, 273–281; Y. I. Aristov, G. Restuccia, G. Cacciola and V. N. Parmon, *Appl. Therm. Eng.*, 2002, **22**, 191–204; N. C. Srivastava and I. W. Eames, *Appl. Therm. Eng.*, 1998, **18**, 707–714; R. Wang and R. Oliveira, *Prog. Energy Combust. Sci.*, 2006, **32**, 424–458; Y. I. Aristov, *Appl. Therm. Eng.*, 2012, **42**, 18–24; B. B. Saha, A. Chakraborty, S. Koyama, K. Srinivasan, K. C. Ng, T. Kashiwagi and P. Dutta, *Appl. Phys. Lett.*, 2007, **91**, 111902; B. B. Saha, S. Jribi, S. Koyama and Yu. I. Aristov, *Int. J. Heat Mass Transfer*, 2009, **52**, 516–524; R. E. Critoph, Z. Tamainot-Telto and S. J. Metcalf, *Int. J. Refrig.*, 2009, **32**, 1212–1229; J. V. Veselovskaya, R. E. Critoph and R. N. Thorpe, *Appl. Therm. Eng.*, 2010, **30**, 1188–1192; K. Habib, B. B. Saha, A. Chakraborty, S. T. Oh and S. Koyama, *Appl. Therm. Eng.*, 2013, **50**, 1582–1589; A. A. Askalany, M. Salem, I. M. Ismael, A. H. H. Ali, M. G. Morsy and B. B. Saha, *Renewable Sustainable Energy Rev.*, 2013, **19**, 565–572.

7 F. Jeremias, D. Fröhlich, C. Janiak and S. Henninger, *New J. Chem.*, 2014, **4**, 24073–24082.

8 J.-P. Zhang, A.-X. Zhu, R.-B. Lin, X.-L. Qi and X.-M. Chen, *Adv. Mater.*, 2011, **23**, 1268–1271.

9 J. J. Low, A. I. Benin, P. Jakubczak, J. F. Abrahamian, S. A. Faheem and R. R. Willis, *J. Am. Chem. Soc.*, 2009, **131**, 15834–15842.

10 C. Heering, I. Boldog, V. Vasylyeva, J. Sanchiz and C. Janiak, *CrystEngComm*, 2013, **15**, 9757–9768.

11 G. Feréy and C. Serre, *Chem. Soc. Rev.*, 2009, **38**, 1380–1399; M. Alhamami, H. Doan and C.-H. Cheng, *Materials*, 2014, **7**, 3198–3250.

12 C. Serre, F. Millange, C. Thouvenot, M. Noguès, G. Marsolier, D. Louër and G. Feréy, *J. Am. Chem. Soc.*, 2002, **124**, 13519–13526.

13 H. Reinsch, M. A. van der Veen, B. Gil, B. Marszalek, T. Verbiest, D. de Vos and N. Stock, *Chem. Mater.*, 2013, **25**, 17–26; H. Reinsch, S. Waitschat and N. Stock, *Dalton Trans.*, 2013, **42**, 4840–4847.

14 K. Brandenburg, *Diamond (Version 3.2), crystal and molecular structure visualization, Crystal Impact*, K. Brandenburg & H. Putz Gbr, Bonn, Germany, 2007–2012.

15 T. Loiseau, C. Serre, C. Huguenard, G. Fink, F. Taulelle, M. Henry, T. Bataille and G. Feréy, *Chem. – Eur. J.*, 2004, **10**, 1373–1382.